Mechanism of Action of *Escherichia coli* Ribonuclease III. Stringent Chemical Requirement for the Glutamic Acid 117 Side Chain and Mn^{2+} Rescue of the Glu117Asp Mutant†

Weimei Sun and Allen W. Nicholson*

Department of Biological Sciences, Wayne State University, 5047 Gullen Mall, Detroit, Michigan 48202

Received January 3, 2001; Revised Manuscript Received February 20, 2001

ABSTRACT: *Escherichia coli* ribonuclease III (EC 3.1.24) is a double-strand- (ds-) specific endoribonuclease involved in the maturation and decay of cellular, phage, and plasmid RNAs. RNase III is a homodimer and requires Mg^{2+} to hydrolyze phosphodiesters. The RNase III polypeptide contains an N-terminal catalytic (nuclease) domain which exhibits eight highly conserved acidic residues, at least one of which (Glu117) is important for phosphodiester hydrolysis but not for substrate binding [Li and Nicholson (1996) *EMBO J. 15,* 1421−1433]. To determine the side chain requirements for activity, Glu117 was changed to glutamine or aspartic acid. The mutant proteins were purified as $(His)_6$-tagged species, and both exhibited normal homodimeric behavior as shown by chemical cross-linking. The Glu117Gln mutant is unable to cleave substrate in vitro under all tested conditions but can bind substrate. The Glu117Asp mutant also is defective in cleavage while able to bind substrate. However, low level activity is observed at extended reaction times and high enzyme concentrations, with an estimated catalytic efficiency ∼15 000-fold lower than that of RNase III. The activity of the Glu117Asp mutant but not that of the Glu117Gln mutant can be greatly enhanced by substituting Mn^{2+} for Mg^{2+}, with the catalytic efficiency of the Glu117Asp−Mn^{2+} holoenzyme ∼400-fold lower than that of the RNase III−Mn^{2+} holoenzyme. For RNase III, a Mn^{2+} concentration of 1 mM provides optimal activity, while concentrations >5 mM are inhibitory. In contrast, the Glu117Asp mutant is not inhibited by high concentrations of Mn^{2+}. Finally, high concentrations of Mg^{2+} do not inhibit RNase III nor relieve the Mn^{2+}-dependent inhibition. In summary, these experiments establish the stringent functional requirement for a precisely positioned carboxylic acid group at position 117 and reveal two classes of divalent metal ion binding sites on RNase III. One site binds either Mg^{2+} or Mn^{2+} and supports catalysis, while the other site is specific for Mn^{2+} and confers inhibition. Glu117 is important for the function of both sites. The implications of these findings on the RNase III catalytic mechanism are discussed.

The maturation and degradation of bacterial RNA involves the coordinated action of a diverse set of cellular ribonucleases. RNA maturation reactions provide functional messenger RNAs and structural RNAs, while degradation pathways can regulate gene expression by controlling mRNA levels, as well as provide mononucleotides for new RNA synthesis (*1*−*3*). A key enzyme in bacterial RNA processing and decay reactions is ribonuclease III (for reviews see refs *1*, *4*, and *5*). RNase[1] III is a double-strand- (ds-) specific endonuclease which is broadly conserved in plants, animals, and fungi as well as in the bacteria (*6*). RNase III of *Escherichia coli* (*7*) has been heavily studied and has served as the prototypical member of the RNase III family. *E. coli* RNase III cleaves the primary transcript of the rRNA operons, creating the immediate precursors to the mature 16S and 23S rRNAs (*8*). While cleavage of the rRNA precursor appears to be a conserved role for RNase III family members, it is also apparent that RNase III is involved in diverse, organism-specific RNA maturation and decay reactions.

E. coli RNase III is active as a homodimer and uses a water molecule as nucleophile to site-specifically cleave phosphodiesters in double-helical structures. Cleavage provides 5′-phosphate, 3′-hydroxyl product termini, and exhaustive digestion of polymeric dsRNA provides short duplex products averaging 12−15 bp in length (*4*, *5*, *9*). RNase III requires a divalent metal ion for activity. Mg^{2+}, Mn^{2+}, Co^{2+}, and Ni^{2+} support substrate cleavage, while Ca^{2+}, Sr^{2+}, and Zn^{2+} are inactive (*4*, *7*, *10*; W. Sun and A. W. Nicholson, unpublished). A divalent metal ion is required for the chemical step but also enhances substrate binding (*10*, *11*). The cleavage sites in *E. coli* RNase III substrates are identified by a combination of double-helical length, base pair sequence, and specific structural elements such as internal loops (*1*, *12*). At physiological salt concentrations in vitro (>160 mM salt, 1−10 mM Mg^{2+}) RNase III can accurately cleave small RNAs which contain the essential set of reactivity epitopes. In low salt and/or in the presence of Mn^{2+}, additional (secondary) cleavage sites are recognized, which are not normally cleaved in vivo (*13*, *14*).

The C-terminal one-third of the *E. coli* RNase III polypeptide contains a dsRNA binding domain (dsRBD) (*15*) (Figure 1). The dsRBD occurs in many other dsRNA binding proteins and consists of an $\alpha\beta\beta\beta\alpha$ fold (reviewed in ref *16*). The

† This work was supported by NIH Grant GM56457.

* Corresponding author. Telephone: 313-577-2862. Fax: 313-577-6891. E-mail: anichol@lifesci.wayne.edu.

[1] Abbreviations: RNase, ribonuclease; DTT, dithiothreitol; DSS, disuccinimidyl suberate; TBE, Tris−borate−EDTA.

10.1021/bi010022d CCC: $20.00
Published on Web 03/28/2001

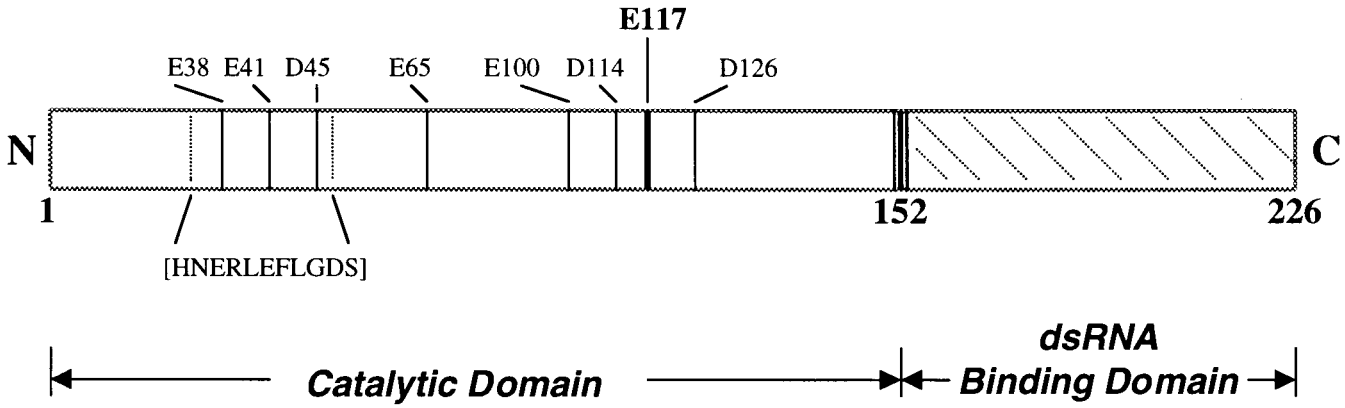

FIGURE 1: *E. coli* RNase III polypeptide. The diagram shows the catalytic (nuclease) domain (residues 1−151; indicated by the open bar), the dsRNA binding domain (residues 152−226; indicated by the hatched bar), and the positions of the highly conserved aspartic acid (D) and glutamic acid (E) residues in the catalytic domain. The sequence HNERLEFLGDS, shown beneath the catalytic domain, is the signature sequence of RNase III family members (*6*, *17*).

dsRBD is important for RNase III recognition and cleavage of substrate in vivo and in vitro (A. K. Amarasinghe, S. Su, W. Sun, R. W. Simons, and A. W. Nicholson, in preparation). The N-terminal two-thirds of the RNase III polypeptide contains the active site, as a truncated form of RNase III specifically lacking the dsRBD can cleave substrate in vitro under specific conditions (W. Sun, E. Jun, and A. W. Nicholson, in preparation). Sequence alignment of RNase III orthologues reveals eight highly conserved aspartic acid or glutamic acid residues within the catalytic domain (*6*, *17*) (Figure 1). These residues are of particular interest, as biochemical and structural studies of other polynucleotidyltransferases have revealed the placement of carboxylic acid side chains in the active site, where they bind divalent metal ion cofactors or serve as proton donor/acceptors (*18*−*20*). The presence of highly conserved residues in the RNase III catalytic domain a priori suggests a conserved mechanism of action of RNase III family members, which has not been described.

There is an increased recognition of the central involvement of dsRNA processing by RNase III family members in gene regulatory pathways, including antisense RNA action, posttranscriptional gene silencing, and RNA interference (RNAi) (e.g., see refs *21* and *22*). In this regard an understanding of the *E. coli* RNase III mechanism of dsRNA recognition and cleavage would have broad ramifications. As part of a goal to determine the catalytic mechanism of *E. coli* RNase III, we are characterizing the functional roles of the conserved aspartic acid and glutamic acid residues in the catalytic domain. We have shown elsewhere (*11*) that mutation of glutamic acid 117 to alanine or lysine selectively blocks phosphodiester hydrolysis without affecting substrate binding affinity or specificity. The Glu117Lys mutation also suppresses RNase III activity in vivo (*23*). Although the behaviors of the Glu117Ala and Glu117Lys mutants demonstrate the importance of the Glu117 side chain, they do not reveal the specific chemical requirements for activity. We describe here the functional consequences of changing Glu117 to glutamine or aspartic acid. We also report the differing abilities of Mg^{2+} and Mn^{2+} to support catalysis by wild-type and mutant RNase III and discuss the implications of these findings on the RNase III mechanism of action.

MATERIALS AND METHODS

Materials. Chemicals and reagents were of reagent grade or molecular biology grade and were obtained from Sigma or Fisher Scientific. Standardized solutions of $MgCl_2$ and $MnCl_2$ were obtained from Sigma. The radiolabeled ribonucleoside 5′-triphosphates [α-^{32}P]UTP (3000 Ci/mmol) and [γ-^{32}P]ATP (3000 Ci/mmol) were from Dupont-NEN (Boston, MA). Ribonucleoside 5′-triphosphates were from Amersham-Pharmacia Biotech (Piscataway, New Jersey). Restriction enzymes, T4 polynucleotide kinase, and Vent DNA polymerase were purchased from New England Biolabs (Beverly, MA) and used according to the supplier's instructions. Calf intestinal alkaline phosphatase was obtained from Roche Molecular Biochemicals (Indianapolis, IN). Plasmid pET-15b was purchased from Novagen (Madison, WI), and *E. coli* strain DH10B was obtained from Life Technologies (Bethesda, MD). T7 RNA polymerase was purified in-house as described (*24*, *25*). Oligodeoxynucleotides used for PCR mutagenesis, and as templates for substrate synthesis (see below), were prepared by the Wayne State Macromolecular Core Facility, or by Life Technologies, and were purified by gel electrophoresis.

RNase III Mutant Protein Overproduction and Purification. The Glu117Gln and Glu117Asp mutations were incorporated into the RNase III (*rnc*) gene by two-step asymmetric PCR (26) essentially as described (*11*). To create the Glu117Gln mutation the GAA (Glu) codon at position 117 was changed to CAA, while for the Glu117Asp mutation the same codon was changed to GAT. The sequence of the Glu117Gln mutagenic oligodeoxynucleotide was 5′-ATTAATGC**[TTG]**GACGGTGTCG-3′. The sequence of the Glu117Asp mutagenic oligodeoxynucleotide was 5′-ATTAATGC**[ATC]**GACGGTGTCG-3′ (the underlined nucleotide in each oligodeoxynucleotide is the mutagenic base, and the bracketed, boldfaced nucleotides indicate the mutated Glu117 codon). Plasmid pET-15b(rnc) (*10*) was used as template, and the sequences of the flanking 5′ and 3′ PCR primers are given elsewhere (*10*, *11*). The amplified, full-length mutant *rnc* gene DNA sequences were purified by agarose gel electrophoresis, cleaved by *Bam*HI and *Nde*I, and ligated to similarly cleaved plasmid pET-15b. Recombinant plasmids were identified by restriction digestion, and

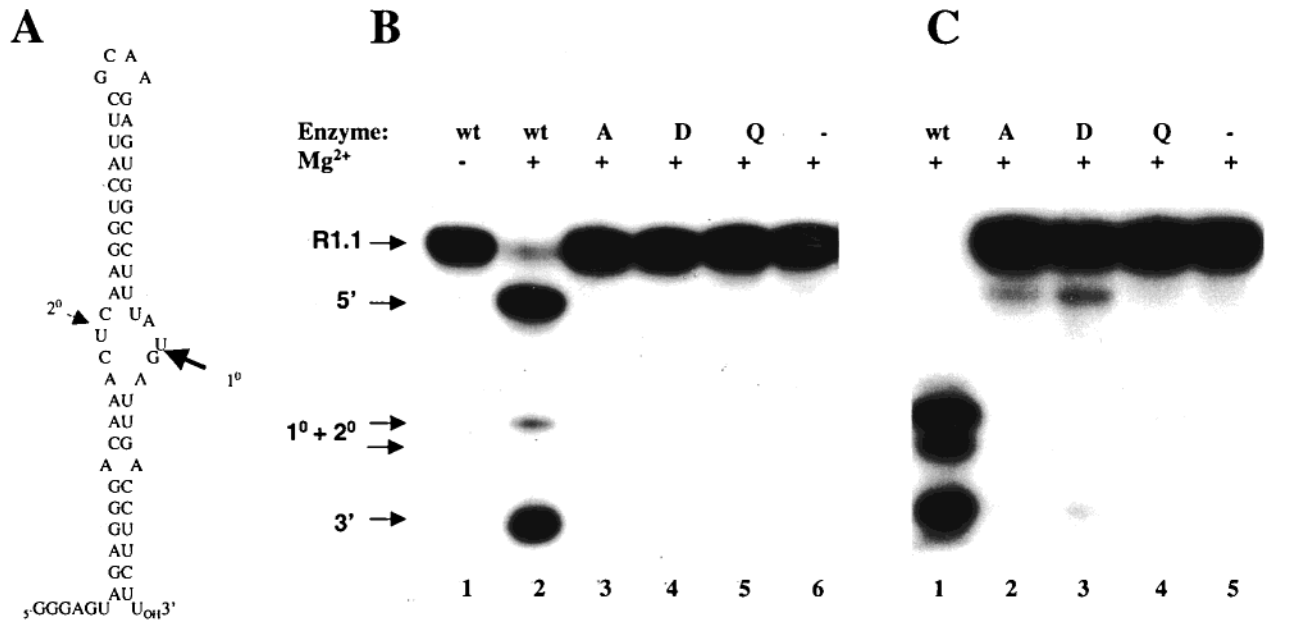

FIGURE 2: (A) Sequence and structure of R1.1 RNA. The primary (1°) and secondary (2°) cleavage sites for RNase III are indicated. (B) Substrate cleavage activity of RNase III (wt) and the Glu117Ala (A), Glu117Asp (D), and Glu117Gln (Q) RNase III mutants. Internally ^{32}P-labeled R1.1 RNA (10 000 cpm; 0.9 pmol) was added to a reaction (20 μL) containing (where indicated) 50 nM protein (dimer concentration) and buffer containing 20 mM $MgCl_2$ (see Materials and Methods). Reactions were initiated by addition of $MgCl_2$ and incubated for 20 min at 37 °C. Reactions were electrophoresed in a 15% polyacrylamide gel and visualized by autoradiography (see Materials and Methods). Lanes: 1, R1.1 RNA incubated with RNase III in the absence of Mg^{2+}; 2, same as lane 1 but in the presence of Mg^{2+}; 3, reaction with the Glu117Ala mutant; 4, reaction with the Glu117Asp mutant; 5, reaction with the Glu117Gln mutant; 6, R1.1 RNA incubated with Mg^{2+} alone. 5′ and 3′ refer to the 47 and 13 nt products of cleavage at the primary site of R1.1 RNA (see panel A). In lane 2, the autoradiographic overexposure (shown here) reveals a small amount of the 28 nt species, generated by cleavage of R1.1 RNA at the secondary site and the primary site. (C) Processing activity of RNase III mutants at high protein concentrations and extended reaction time. Reactions (set up as described above) were incubated at room temperature for 20 h using 500 nM enzyme. Lanes: 1, reaction with RNase III (in these conditions the R1.1 RNA primary and secondary sites are both fully cleaved); 2, reaction with the Glu117Ala mutant; 3, reaction with the Glu117Asp mutant; 4, reaction with the Glu117Gln mutant; 5, reaction with Mg^{2+} alone.

the mutations were verified by sequencing of both DNA strands.

The RNase III mutants were overproduced in *E. coli* strain BL21(DE3)*rnc105,recA*. This strain is described elsewhere (*27*) and permits overproduction and purification of RNase III mutants free of endogeneous RNase III activity. Specifically, the *rnc105* mutation changes Gly44 to Asp in the chromosomally located *rnc* gene and completely abolishes RNase III activity (*28*, *29*). Briefly, cells containing plasmid were grown in LB + ampicillin (100 μg/mL) at 37 °C to an OD (600 nm) of ~0.3−0.4 and then treated with 0.5 mM IPTG. Cultures were incubated for an additional 4 h with vigorous aeration. The cells were harvested by centrifugation and stored at −20 °C prior to further processing. The RNase III mutants were purified from the supernatant fraction of sonicated cell lysates using Ni^{2+} affinity columns (HisBind resin, Novagen) as described elsewhere (*27*). Separate affinity columns were used for each mutant as well as for wild-type RNase III. The purified proteins were stored at −20°C in 0.5 M NaCl, 30 mM Tris-HCl (pH 7.9), 0.5 mM DTT, 0.5 mM EDTA, and 50% glycerol. SDS−PAGE analysis revealed the proteins to be at least 90% pure, and cleavage assays (see below) established that the preparations were free from contaminating nuclease activities. The yield of purified protein was 4, 8, and 1 mg/L of culture for $(His)_6$-RNase III, $(His)_6$-Glu117Asp, and $(His)_6$-Glu117Gln proteins, respectively. Since the N-terminal $(His)_6$ tag has a negligible effect on RNase III activity (*27*), it is therefore assumed that the $(His)_6$ tag also does not differentially affect the activity of the Glu117Gln and Glu117Asp mutants. For the purposes of this report, $(His)_6$-RNase III (or mutant) will be referred to as RNase III (or mutant).

Substrate Synthesis. The processing substrate R1.1 RNA (Figure 2A) was synthesized using T7 RNA polymerase and an oligodeoxynucleotide template according to a standard protocol (*30*), with modifications as described (*27*). Internally ^{32}P-labeled R1.1 RNA was prepared by including [α-^{32}P]-UTP (final specific activity 100 Ci/mol) in the reaction. To prepare 5′-^{32}P-labeled R1.1 RNA, unlabeled trancript was dephosphorylated with calf intestine alkaline phosphatase and then treated with [γ-^{32}P]ATP (3000 Ci/mmol) and T4 polynucleotide kinase. RNAs were purified by electrophoresis in polyacrylamide/7 M urea gels as described (*27*) and stored in TE buffer (pH 7.5) at −20 °C.

Substrate Cleavage Assay. Cleavage assays were performed at 37 °C essentially as described (*27*) using internally ^{32}P-labeled R1.1 RNA and a potassium glutamate buffer (*10*). We have shown that glutamate anion extends the upper range of salt concentrations over which RNase III processing of substrate can efficiently occur (*10*). In this study the potassium glutamate concentration was the same in all assays (250 mM) and therefore was not a variable. Reaction times and protein concentrations (reported as dimer form) are provided in the appropriate figure or table legend. Reactions were analyzed by electrophoresis in a 15% polyacrylamide gel containing 7 M urea and quantitated by radioanalytic imaging (Ambis) or by phosphorimaging (Storm 860, Molecular Dynamics) as described (*27*) (see also legend to Table

Table 1: Substrate Binding Affinities and Steady-State Catalytic Parameters for RNase III and the Glu117Gln and Glu117Asp RNase III Mutants

		RNase III	Glu117Asp	Glu117Gln
	Substrate Binding Affinities			
	K'_D (nM)[a]	1.8	1.1	0.8
	Catalytic Parameters[b]			
$+Mg^{2+}$	k_{cat} (min^{-1})	3.8	ND	nd
	K_m (nM)	335	ND	nd
	k_{cat}/K_m ($M^{-1}\,min^{-1}$)	1.1×10^7	$[7.2 \times 10^2]$[c]	nd
$+Mn^{2+}$	k_{cat} (min^{-1})	1.4	2.1×10^{-2}	nd
	K_m (nM)	110	641	nd
	k_{cat}/K_m ($M^{-1}\,min^{-1}$)	1.3×10^7	3.3×10^4	nd

[a] Proteins were purified as described in Materials and Methods. Gel shift assays were performed using 5′-^{32}P-labeled R1.1 RNA, with the buffer supplemented with 5 mM $CaCl_2$. The apparent (nonequilibrium) dissociation constants (K'_D values) were determined as described (*11*) by least-squares curve fitting (KaleidaGraph). The reported values are the average of three or more separate experiments, with the standard error for each ≤25%. The K'_D of 1.8 nM for the RNase III−R1.1 RNA complex (5 mM Ca^{2+}) is in excellent agreement with the previously determined value of 1.8 nM (*11*). [b] Cleavage assays were performed as described in Materials and Methods using 10 nM enzyme (dimer concentration) and internally ^{32}P-labeled R1.1 RNA. Assays with $MgCl_2$ used a 5 mM metal ion concentration, while assays with $MnCl_2$ used a 1 mM concentration (for RNase III) or 100 mM concentration (for Glu117Asp). We have shown elsewhere (*10*) that RNase III cleavage of substrate follows Michaelis−Menten steady-state kinetics (*39*), wherein reversible binding of substrate is followed by the chemical step (hydrolysis) and product release. The K_m and k_{cat} values were determined by nonlinear least-squares analysis (Kaleidagraph), and the reported values are the average of three experiments. The standard errors for the k_{cat} values were all <15%. The standard errors for the K_m values were all ≤20%, except for RNase III (1 mM Mn^{2+}), which was ±40%. The previously determined K_m and k_{cat} values for native RNase III [i.e., without the $(His)_6$ tag, in 10 mM Mg^{2+}] are 330 nM and 1.8 min^{-1}, respectively (*10*). ND = not determined; nd = not detectable. [c] The catalytic efficiency (k_{cat}/K_m) for the RNase III Glu117Asp−Mg^{2+} mutant holoenzyme was estimated as follows. The initial rate of cleavage of R1.1 RNA by the Glu117Asp mutant was determined in the presence of 5 mM $MgCl_2$ (5 h reaction time, 500 nM enzyme) and compared to the initial rate of Glu117Asp mutant cleavage of R1.1 RNA in the presence of 100 mM $MnCl_2$ (10 min reaction time, 500 nM enzyme). The latter conditions were sufficient to allow determination of the k_{cat} and K_m values, which are provided in the table. Since the substrate concentrations used are significantly lower than the K_m, the ratio of initial cleavage rates is therefore approximately equal to the ratio of the catalytic efficiencies (*40*).

1). Curve fitting for determination of kinetic parameters was carried out using KaleidaGraph software (v 3.5) (see also appropriate table and figure legends).

Substrate Binding Assay. Gel mobility shift assays were performed as described (*11*, *27*) using 5′-^{32}P-labeled R1.1 RNA. Gel shift reaction buffers, gel buffer, and electrophoresis buffer were supplemented with 5 mM $CaCl_2$. Samples were electrophoresed at 5 °C in a 6% polyacrylamide gel containing TBE buffer (+5 mM $CaCl_2$) and were quantitated by radioanalytic imaging or by phosphorimaging (*11*, *12*) (see also legend to Table 1). Nonequilibrium dissociation constants (K'_D values) were determined by curve fitting using KaleidaGraph software (see also appropriate figure and table legends).

RESULTS

The importance of glutamic acid 117 was first indicated by the ability of the Glu117Lys mutation to suppress RNase III processing activity in vivo (*5*, *23*). A functional role for this residue in the catalytic mechanism was suggested by the ability of the Glu117Lys mutation or the Glu117Ala mutation to block phosphodiester cleavage in vitro without inhibiting substrate binding (*13*, *23*). To gain more information on the chemical requirements for activity at this position, we created the Glu117Gln and Glu117Asp mutants. The glutaminyl side chain is isosteric with the glutamate side chain and possesses similar polarity and hydrogen bonding capacity. However, the amide group cannot act as an acid or base and has a significantly weakened affinity for divalent metal ions (*20*, *31*). The aspartyl side chain retains the carboxylic acid but with its position shifted by a methylene group (∼1.5 Å). Both mutations represent minimal structural changes but have the potential for a significant effect on catalytic activity.

The Glu117Gln and Glu117Asp mutants were overproduced as $(His)_6$-tagged polypeptides in an *E. coli* DE3 strain containing a chromosomal mutation that suppresses endogenous RNase III activity (see Materials and Methods). The mutant proteins could be overproduced at high levels, and both were present in the soluble portion of sonicated cell extracts. There was no significant inhibitory effect of protein overproduction on cell growth. The solubility of the mutant proteins was suggestive of proper protein folding. The proteins were purified on Ni^{2+} affinity columns. Analysis by SDS−PAGE revealed similar apparent molecular masses (∼29 kDa; data not shown). To test for dimeric behavior, the purified RNase III mutants were treated with the amine-specific protein cross-linker DSS. This reagent was used previously to confirm the dimeric behavior of RNase III, as well as to establish the dimeric behaviors of the Glu117Ala and Glu117Lys mutants (*11*). The cross-linked dimeric forms (∼58 kDa) of the Glu117Gln and Glu117Asp polypeptides were detectable by SDS−PAGE, and the cross-linking efficiencies were essentially the same as that seen with RNase III (data not shown). In summary, the purification and cross-linking behaviors indicate that the Glu117Gln and Glu117Asp mutants exhibit closely similar physical properties as RNase III.

The Glu117 → Gln Mutation Blocks Phosphodiester Hydrolysis without Inhibiting Substrate Binding. The Glu117Gln mutant was tested for its ability to cleave substrate in vitro. R1.1 RNA (Figure 2A) is based on the bacteriophage T7 phage R1.1 processing signal, which is located between genes 1 and 1.1 in the T7 genetic early region (*32*). RNase III cleavage of the T7 polycistronic early mRNA precursor at the indicated phosphodiester within the internal loop creates the mature 5′ and 3′ ends of the flanking mRNAs (*32*). The 60 nt R1.1 RNA is efficiently cleaved in vitro at the canonical site by purified RNase III (*33*, *34*). The cleavage assay employed physiologically relevant salt conditions (10 mM Mg^{2+}, 250 mM potassium glutamate) (*10*), and substrate was in excess of enzyme to establish steady-state conditions. The assay results reveal that the Glu117Gln mutant is unable to cleave R1.1 RNA (Figure 2B, lane 5) under conditions where RNase III carries out efficient processing (Figure 2B, lane 2). The lack of activity of the Glu117Gln mutant under these conditions is similar to the previously described (*11*) Glu117Ala mutant (Figure 2B, lane 3). The Glu117Gln mutant did not exhibit any activity over a wide range of Mg^{2+} concentrations (data not shown) or at high protein concentrations and extended

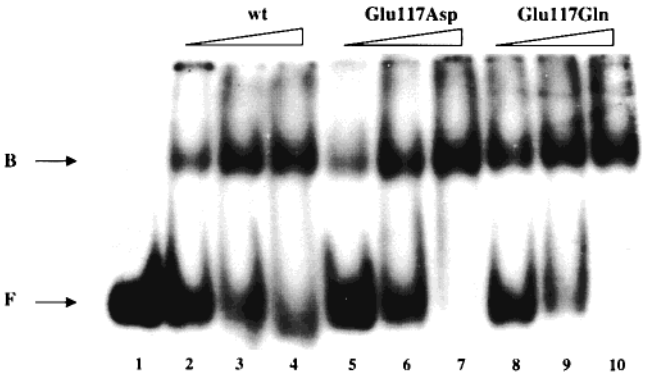

FIGURE 3: Substrate binding activity of the Glu117Asp and Glu117Gln mutants. The gel shift assay was performed as described in Materials and Methods, using 5′-^{32}P-labeled R1.1 RNA (10^4 cpm; 1.5 fmol) and including $CaCl_2$ (5 mM) in the binding reactions. Reactions (20 μL) were electrophoresed in a nondenaturing, 6% polyacrylamide gel containing 5 mM $CaCl_2$ and were visualized by autoradiography. F refers to the free (unbound) R1.1 RNA, and B indicates the bound (protein-shifted) R1.1 RNA. Lanes: 1, no protein added; 2−4, 1.45, 2.9, and 14.5 nM RNase III (wt), respectively; 5−7, 1.45, 2.9, and 14.5 nM Glu117Asp mutant, respectively; 8−10, 1.45, 2.9, and 14.5 nM Glu117Gln mutant, respectively.

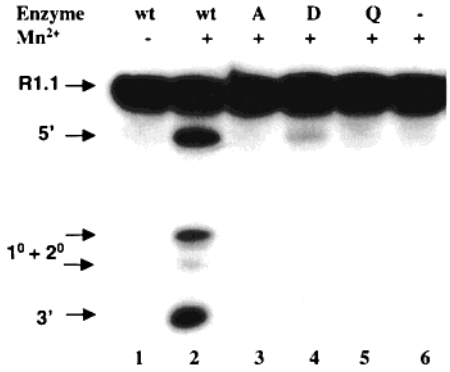

FIGURE 4: Manganous ion enhancement of Glu117Asp RNase III mutant activity. The cleavage reactions used internally ^{32}P-labeled R1.1 RNA (15 000 cpm, 1.3 pmol) in a 20 μL reaction containing 50 nM enzyme and 20 mM $MnCl_2$. Reactions were initiated by addition of $MnCl_2$, incubated for 20 min at 37 °C, and electrophoresed in a 15% polyacrylamide/7 M urea gel. Reactions were visualized by autoradiography. Lanes: 1, RNase III (wt) incubated with substrate without Mn^{2+}; 2, same as lane 1 but with 20 mM Mn^{2+} [this experiment also shows that Mn^{2+} supports cleavage at the R1.1 RNA secondary site (compare with lane 2, Figure 2B)]; 3, reaction with Glu117Ala (A) mutant; 4, reaction with Glu117Asp (D) mutant (in this experiment the 3′-end-containing cleavage product (3′) is just visible); 5, reaction involving Glu117Gln (Q); 6, R1.1 RNA incubated with 20 mM Mn^{2+} in the absence of protein.

reaction times. Thus, incubation of ^{32}P-labeled R1.1 RNA with the Glu117Gln mutant (500 nM) at room temperature for 20 h (20 mM Mg^{2+}) did not provide cleavage of substrate that was detectable over background (Figure 2C, lane 4). Interestingly, under these conditions the Glu117Ala mutant exhibited low-level cleavage activity (Figure 2C, lane 2).

The lack of catalytic activity of the Glu117Gln mutant could reflect an inability to bind substrate. Alternatively, substrate binding is retained but with the cleavage step blocked. A gel mobility shift assay was used to distinguish between these alternatives. In the assay Mg^{2+} was replaced by Ca^{2+} to prevent cleavage by RNase III while promoting substrate binding (*11*). The assay results (Figure 3) reveal that the Glu117Gln mutant binds R1.1 RNA to form a protein−RNA complex with mobility and stability similar to that involving RNase III (compare lanes 8−10 with lanes 2−4, Figure 3). Protein titration−gel shift assays were performed to determine the apparent dissociation constant (K'_D) for the Glu117Gln−R1.1 RNA complex, which is provided in Table 1. The K'_D of 0.8 nM indicates a comparable, if in fact not slightly greater stability of the Glu117Gln−R1.1 RNA complex compared to the RNase III−R1.1 RNA complex (K'_D of 1.8 nM). We conclude that converting the glutamic acid 117 side chain to a glutaminyl side chain does not inhibit substrate binding.

The Glu117 → Asp Mutation Also Inhibits Phosphodiester Hydrolysis without Affecting Substrate Binding. The Glu117-Asp mutant also is defective in its ability to cleave R1.1 RNA (Figure 2B, lane 4). However, in contrast to the Glu117Gln mutant, a small amount of substrate cleavage can be observed using 500 nM protein, 20 mM Mg^{2+}, and a 20 h reaction time (Figure 2C, lane 3). The identical pattern of products indicates that the methylene shift does not alter the site specificity of cleavage. The low-level activity of the Glu117Asp mutant was not increased by raising the Mg^{2+} concentration to 200 mM (data not shown). Although the cleavage activity was too low to allow accurate determination of initial rates, a catalytic efficiency of 7.2×10^2 $M^{-1}min^{-1}$ for the Glu117Asp−Mg^{2+} holoenzyme could be indirectly determined (see Table 1 legend), which is ∼15 000-fold lower than the RNase III−Mg^{2+} holoenzyme. The gel shift assay (Figure 3, lanes 5−7) reveals that the Glu117Asp mutant efficiently binds R1.1 RNA, and the K'_D of 1.1 nM (Table 1) is similar to the K'_D for RNase III. We conclude that the methylene shift severely but not completely inhibits the catalytic activity of RNase III while not affecting substrate binding.

Manganous Ion Greatly Enhances the Catalytic Activity of the Glu117 → Asp Mutant. The defective activities of the Glu117Gln and Glu117Asp RNase III mutants indicate the stringent catalytic requirement for a glutamic acid side chain. Since RNase III can use other divalent metal ions, including Mn^{2+}, Co^{2+}, and Ni^{2+} (*10*), we tested whether the activities of either mutant could be supported by these species. A cleavage assay reveals that the Glu117Gln mutant is inactive in the presence of Mn^{2+} (Figure 4, lane 5) as well as in the presence of Co^{2+}, Ca^{2+}, Ni^{2+}, Sr^{2+}, or Zn^{2+} (data not shown). In contrast, Mn^{2+} supports substrate cleavage by the Glu117Asp mutant, albeit to a significantly lower extent than the RNase III-catalyzed reaction (Figure 4, compare lanes 4 and 2). A control experiment (Figure 4, lane 6), shows that Mn^{2+} alone does not cleave R1.1 RNA. R1.1 RNA cleavage by the Glu117Asp−Mn^{2+} mutant holoenzyme provides the same 5′-end-containing product as that of the RNase III−Mn^{2+} holoenzyme reaction (Figure 4, compare lanes 2 and 4; the 3′ product in lane 4 is only visible following autoradiographic overexposure). The experiment also shows that Mn^{2+} strongly promotes RNase III cleavage at the secondary site of R1.1 RNA, as well as at the primary site (Figure 4, lane 2: "1° + 2°" species). Mn^{2+}-enhanced cleavage of secondary sites has been described elsewhere (*10*, *14*). Interestingly, secondary site cleavage is not observed with the Glu117Asp−Mn^{2+} mutant holoenzyme (Figure 4, lane 4).

We examined substrate cleavage by RNase III and the Glu117Asp mutant as a function of divalent metal ion type and concentration. For RNase III, Mg^{2+} and Mn^{2+} provide strikingly different activity versus metal ion concentration profiles. In the presence of Mg^{2+} the initial cleavage rate reaches a plateau by ~2 mM metal ion, with a calculated apparent dissociation constant (K_{app}) of 0.6 mM (Figure 5A,B). In the presence of Mn^{2+} the maximum rate is attained by ~1 mM and then sharply decreases at higher concentrations (Figure 5C,D). The biphasic behavior of Mn^{2+} indicates two functional classes of metal ion sites: one supporting catalysis and the other conferring inhibition (see below). Since RNase III cleavage of substrate obeys Michaelis−Menten kinetics (*10*), the catalytic parameters (K_m, k_{cat}) for the RNase III−Mg^{2+} and RNase III−Mn^{2+} holoenzymes were determined by measuring the initial rate of substrate cleavage as a function of substrate concentration. The catalytic efficiency (k_{cat}/K_m) of RNase III in the presence of Mg^{2+} (5 mM) or Mn^{2+} (1 mM) is essentially identical (1.1×10^7 M^{-1} min^{-1} and 1.3×10^7 M^{-1} min^{-1}, respectively) (Table 1). RNase III therefore cleaves substrate with the same efficiency at the optimal concentrations of Mg^{2+} or Mn^{2+}. The lower k_{cat} for the Mn^{2+}-supported reaction relative to the Mg^{2+}-supported reaction is balanced by a correspondingly lower K_m, which suggests that Mn^{2+} enhances substrate binding while slowing the rate of one or more steps occurring in the enzyme−substrate complex (see Discussion).

The Glu117Asp mutation abolishes the inhibitory action of Mn^{2+}. Thus, increasing the Mn^{2+} concentration to 100 mM provides an increase in substrate cleavage, without apparent inhibition (Figure 5E,F). Thus, the glutamic acid 117 side chain is not only required for catalysis but is also important for Mn^{2+} inhibition. The calculated K_{app} for Mn^{2+} is 38 mM (Figure 5F), and the Glu117Asp−Mn^{2+} holoenzyme exhibits substrate saturation kinetics (Figure 6). The K_m and k_{cat} values for the Glu117Asp−Mn^{2+} holoenzyme are provided in Table 1. The catalytic efficiency of 3.3×10^4 M^{-1} min^{-1} (in the presence of 100 mM Mn^{2+}) establishes that Mn^{2+} does not provide a full rescue of processing activity. The behavior of the Glu117Asp−Mn^{2+} holoenzyme indicates that Mn^{2+} inhibition of RNase III is not due to an interaction of metal ion with substrate. If this were the case, inhibition would occur independent of protein structure. Moreover, the inability of high Mg^{2+} concentrations to inhibit RNase III (Figure 5A,B) or to relieve the Mn^{2+} imposed inhibition (see below) also does not support an inhibitory interaction of metal ion and substrate.

Excess Mg^{2+} Does Not Relieve Mn^{2+} Inhibition of RNase III. The cleavage assays indicate two functional classes of divalent metal ion binding sites. Occupancy of the higher affinity site by Mn^{2+} (or Mg^{2+}) promotes catalysis, while occupancy of the second site by Mn^{2+} confers inhibition. The inability of high Mg^{2+} concentrations to inhibit cleavage could either reflect an inability of Mg^{2+} to bind to the inhibitory site or to a lack of an inhibitory effect of bound Mg^{2+}. To distinguish between these possibilities, we performed cleavage assays in the presence of metal ion mixtures, wherein the amount of substrate cleavage was measured as a function of the Mg^{2+}/Mn^{2+} ratio. In one experiment the Mg^{2+} concentration was fixed at 0.5 mM, and increasing amounts of Mn^{2+} were added to the reaction. The results (Figure 7A) show that Mn^{2+} can still inhibit cleavage in the presence of Mg^{2+}. Essentially the same results were obtained when the experiment was performed using either 5 or 50 mM Mg^{2+} (data not shown). In the second experiment the Mn^{2+} concentration was fixed at 20 mM, selected to confer strong inhibition, and Mg^{2+} was added in increasing amounts. The results (Figure 7B) show that increasing the Mg^{2+} concentration to 50 mM does not relieve the Mn^{2+} inhibition. These data indicate that Mg^{2+} does not recognize the Mn^{2+} inhibitory site.

DISCUSSION

This study has demonstrated the stringent functional requirement for a glutamic acid side chain at position 117 in the *E. coli* RNase III polypeptide. The inactivity of the Glu117Gln mutant establishes the importance of the carboxylic acid group functionality, while the severely reduced activity of the Glu117Asp mutant demonstrates the requirement for precise positioning. The data are consistent with an active site location for the Glu117 side chain and that the carboxylic acid group may interact with one or perhaps two divalent metal ions. Thus, the Glu117Gln and Glu117Asp mutations, as well as the previously characterized Glu117Lys and Glu117Ala mutations (*11*), do not affect protein solubility or dimeric structure, indicating a localized inhibitory effect. Second, the two mutations inhibit the chemical step without affecting substrate binding. Third, the inability of either Mg^{2+} or Mn^{2+} to rescue the activity of the Glu117Gln mutant is consistent with the weak affinity of the carboxamide group for divalent metal ions (*20*, *31*). Fourth, the requirement for precise positioning of the carboxyl group is consistent with the strict stereochemical demands placed on active site residues in order to provide maximal catalytic rate enhancement. Fifth, the ability of Mn^{2+} to partially restore the loss of activity caused by the Glu → Asp methylene shift may reflect the higher relative affinity of Mn^{2+} for oxygen ligands (occurring in both substrate and enzyme) which may serve to stabilize a catalytic enzyme−substrate complex (*20*, *35*). Nonetheless, the ability of Mn^{2+} to functionally complement the Glu117Asp mutation does not prove a direct metal ion−Glu117 interaction, which awaits a structural analysis.

On the Mechanism of Mn^{2+} Inhibition of RNase III. RNase III is similar to many other phosphodiesterases in its catalytic requirement for a divalent metal ion. It is most likely that Mg^{2+} is the preferred cofactor, due to its relative intracellular abundance (~1−5 mM) and since RNase III attains optimal activity by ~2 mM Mg^{2+}. However, it has been known since the original characterization of RNase III (*7*) that Mn^{2+} in the 0.1−1 mM concentration range can support substrate cleavage, while higher concentrations (>5 mM) are inhibitory. We have extended this observation to show that there are two functional classes of Mn^{2+} binding sites on RNase III. One site activates phosphodiester hydrolysis and can use Mn^{2+} or Mg^{2+} with comparable efficiency. This site is most likely in the catalytic site and for the purposes of this discussion will be termed the activator (A) site. The A site also can use Ni^{2+} or Co^{2+} as functional species (*10*; W. Sun and A. W. Nicholson, unpublished). Replacing Mg^{2+} by Mn^{2+} decreases both the K_m, and k_{cat}, which yields a catalytic efficiency of the RNase III−Mn^{2+} holoenzyme similar to that of the RNase III−Mg^{2+} holoenzyme. The divalent metal ion stoichiometry required for catalysis is under study.

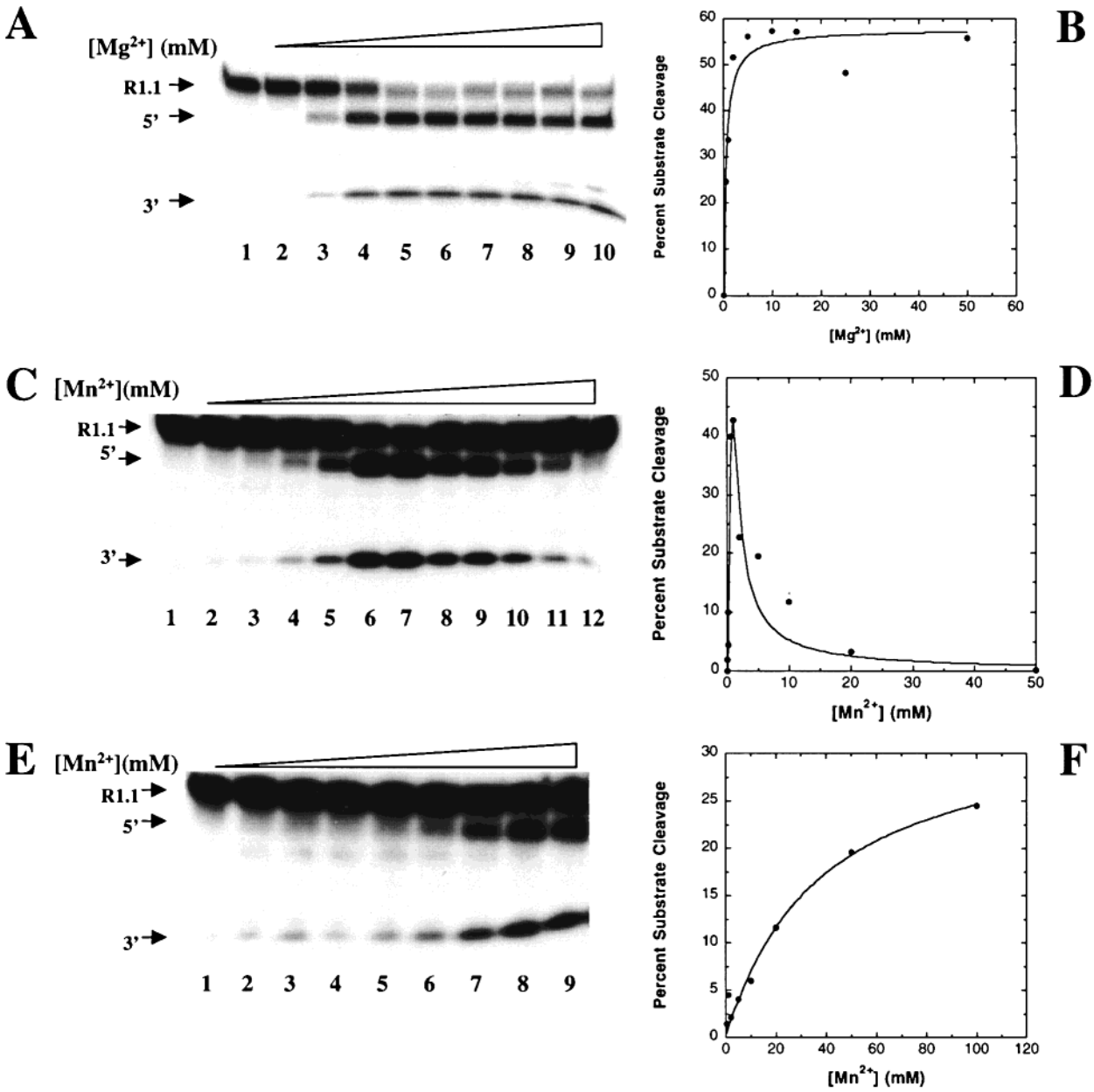

FIGURE 5: Divalent metal ion concentration dependence of substrate cleavage by RNase III and the Glu117Asp RNase III mutant. Cleavage reactions (20 μL) involved internally ^{32}P-labeled R1.1 RNA and 50 nM enzyme (dimer concentration). Reactions were initiated by addition of metal ion (concentrations given below), incubated for 6 min at 37 °C, then stopped with EDTA, and electrophoresed in a polyacrylamide/7 M urea gel (see Materials and Methods). Reactions were visualized by autoradiography, and the extent of substrate cleavage was quantitated by radioanalytic imaging (Ambis). In panels B, D, and F, the data from the experiments shown in panels A, C, and E, respectively, were fitted to curves which corresponded to either a single affinity class of binding site (panels B and F) or two affinity classes of sites (panel D), one of which confers inhibition (I site) (see also Discussion). No assumption was made regarding the number of metal ions binding to a given site. For the purposes of the curve fitting in panel D, it was assumed that Mn^{2+} binding to the I site completely inhibits cleavage in the steady state (see also Discussion). (A) RNase III cleavage of substrate as a function of Mg^{2+} concentration. The positions of the substrate (R1.1) and the 5′- and 3′-end-containing cleavage products (5′ and 3′, respectively) are indicated on the left side. Lanes: 1, 5 mM Mg^{2+}, no enzyme added; 2, 50 nM RNase III without Mg^{2+}; 3−10, 50 nM RNase III and 0.5, 1, 2, 5, 10, 15, 25, and 50 mM Mg^{2+}, respectively. (B) RNase III activity as a function of Mg^{2+} concentration. Based on the best fit curve, the apparent dissociation constant for Mg^{2+} is 0.56 ± 0.15 mM. (C) RNase III activity as a function of Mn^{2+} concentration. Lanes: 1, R1.1 incubated with 1 mM Mn^{2+} in the absence of RNase III; 2, R1.1 RNA incubated with RNase III (50 nM) in the absence of Mn^{2+}; 3−12, 0.05, 0.1, 0.2, 0.5, 1, 2, 5, 10, 20, and 50 mM Mn^{2+}, respectively. (D) Percent cleavage as a function of Mn^{2+} concentration. The data did not permit unambiguous determination of apparent dissociation constants for Mn^{2+} binding to the activator (A) and inhibitor (I) sites. (E) Glu117Asp RNase III mutant activity as a function of Mn^{2+} concentration. Reactions (20 μL) included 50 nM enzyme and 10^4 cpm (0.87 pmol) of R1.1 RNA. Reactions were initiated by addition of Mn^{2+} and incubated for 4 min at 37 °C. Lanes: 1, 1 mM Mn^{2+} and R1.1 RNA without enzyme; 2−9, 50 nM Glu117Asp mutant and 0.5, 1, 2, 5, 10, 20, 50, or 100 mM Mn^{2+}. Note the absence of R1.1 RNA cleavage at the secondary site (see Discussion). (F) Percent substrate cleavage by the Glu117Asp mutant as a function of Mn^{2+} concentration. The Mn^{2+} concentration which provides the half-maximal rate of cleavage is 38 ± 11 mM.

The second site is specific for Mn^{2+} and confers inhibition. The inhibitory (I) site is located on the enzyme rather than on substrate. Thus, if inhibition were due to a Mn^{2+}−substrate interaction, then excess Mg^{2+} would be expected to relieve the inhibition, which is not observed. Second, the sustained activity of the Glu117Asp mutant at high Mn^{2+}

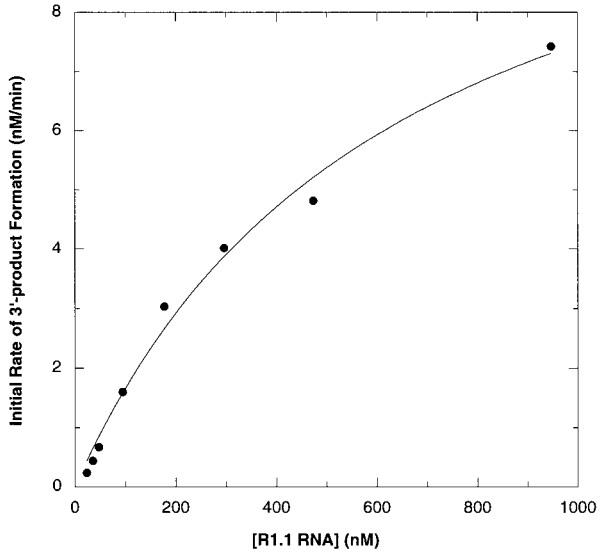

FIGURE 6: Initial rate of R1.1 RNA cleavage by the Glu117Asp−Mn^{2+} holoenzyme (100 mM Mn^{2+}) as a function of substrate concentration. Reactions included 500 nM Glu117Asp mutant (dimer concentration) and were for 10 min at 37 °C. Reactions were electrophoresed in a 15% polyacrylamide/7 M urea gel and quantitated by radioanalytic imaging. Curve fitting was carried out assuming Michaelis−Menten kinetics. The K_m and k_{cat} values are provided in Table 1.

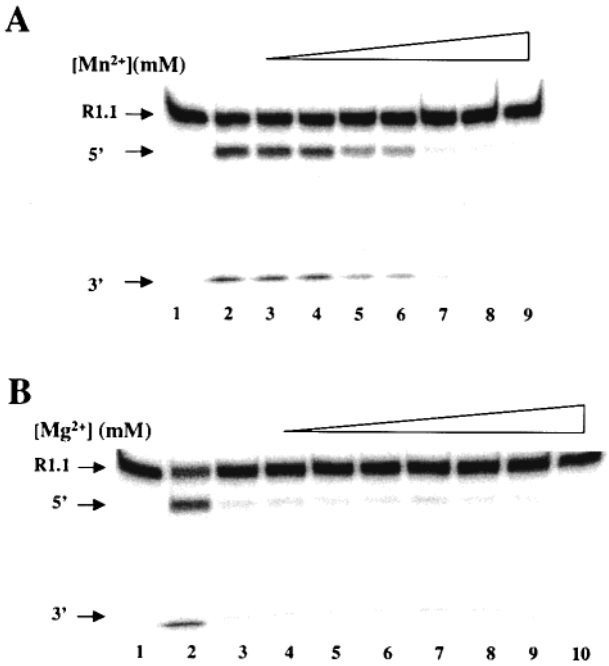

FIGURE 7: Excess Mg^{2+} does not relieve Mn^{2+} inhibition of RNase III. Substrate cleavage reactions used internally ^{32}P-labeled R1.1 RNA, and 10 nM RNase III (dimer concentration) and were for 2 min. (A) Mn^{2+} inhibition of R1.1 RNA cleavage in the presence of 0.5 mM Mg^{2+}. Lane 1 contains 0.5 mM $MgCl_2$ without enzyme. Lane 2 is the same as lane 1 but includes RNase III. Lanes 3−9 are the same as lane 2 but with increasing concentrations of $MnCl_2$ (0.5, 1.0, 2.0, 5.0, 10, 20, and 50 mM, respectively). (B) Excess Mg^{2+} does not relieve Mn^{2+} inhibition of cleavage. Cleavage reactions included 20 mM Mn^{2+}, which confers strong inhibition (see Figure 5B). Lanes: 1, R1.1 RNA incubated with 20 mM $MnCl_2$ in the absence of RNase III; 2, reaction containing 1 mM $MnCl_2$ and RNase III; 3−10, reaction containing 20 mM Mn^{2+} and increasing concentrations of $MgCl_2$ (0, 0.5, 1.0, 2.0, 5.0, 10, 20, and 50 mM, respectively).

concentrations is inconsistent with the substrate as the inhibitory target. Third, using other RNase III substrates with structures different from that of R1.1 RNA provides the same Mn^{2+} inhibitory behavior (W. Sun and A. W. Nicholson, unpublished experiments). Since binding of Mn^{2+} to the I site inhibits substrate cleavage in the steady state, inhibition therefore could be due to an increase in K_m and/or decrease in k_{cat}. Alternatively, the product release rate could be retarded. Preliminary experiments (W. Sun and A. W. Nicholson, unpublished) indicate that 50 mM Mn^{2+} does not inhibit substrate cleavage in single-turnover conditions, suggesting that Mn^{2+} occupancy of the I site inhibits product release. In this respect, an enhanced affinity for product can be mirrored by an enhanced affinity for substrate, which is suggested by the lower K_m for the RNase III−Mn^{2+} holoenzyme relative to that of the RNase III−Mg^{2+} holoenzyme (Table 1). Despite the intriguing activation−inhibition behavior conferred by Mn^{2+}, there is no reason yet to believe that this metal ion controls RNase III activity in vivo. The intracellular concentration of Mn^{2+} is in the low micromolar range, and significant inhibition of RNase III only occurs at Mn^{2+} concentrations greater than 5 mM.

Involvement of Glu117 in both Mn^{2+}-Dependent Activation and Inhibition of RNase III and Implications for the Catalytic Mechanism. The Mn^{2+} concentration dependence of Glu117-Asp mutant activity (Figure 5F) suggests that the methylene shift significantly weakens the affinity of the A site for Mn^{2+} (and perhaps also for Mg^{2+}, although the activity was too low to be measured with confidence). Since mutation of Glu117 to Asp also abrogates the inhibitory action of Mn^{2+}, the glutamic acid side chain is also important for I site function. One possibility is that the A and I sites are in close proximity, such that Glu117 can simultaneously interact with the metal ions bound to each site. The existence of an inhibitor and activator site for Mn^{2+} and the effects of the Glu117 mutations reveal an intriguing similarity between RNase III and *E. coli* RNase H1. Thus, RNase H1 activity is supported by either Mg^{2+} or Mn^{2+} and is also inhibited by high Mn^{2+} concentrations (*36*). Second, a recent structural analysis of *E. coli* RNase H1 (*37*) reveals that Mn^{2+} binds to two sites on the enzyme, with one metal ion in the active site and the other occupying an "attenuator" (i.e., inhibitor) site. The two metal ions are separated by 4 Å, and a highly conserved aspartic acid (Asp10) bridges the two sites and interacts with both metal ions (*37*). Although there is no obvious sequence similarity between RNase III and RNase H1, we note that there also is little sequence similarity between RNase H orthologues or between RNase H and other polynucleotidyl transferases whose physical structures contain highly similar arrays of carboxylic acid side chains in the active sites (*18*−*20*, *38*). Both RNase III and RNase H1 recognize double-helical nucleic acids, and both hydrolyze phosphodiesters in a divalent metal ion-dependent manner, providing 5′-phosphate, 3′-hydroxyl product termini. It is therefore possible that RNase III and RNase H1 have similar active site structures and employ similar if not identical hydrolytic mechanisms. We are carrying out enzymological analyses of additional RNase III mutants to test this intriguing possibility.

ACKNOWLEDGMENT

We thank Dr. A. Harmouch for providing T7 RNA polymerase and Drs. D. R. Evans and R. H. Nicholson for

comments on the manuscript. We also appreciate collaboration with and input from Dr. R. W. Simons (UCLA). We gratefully acknowledge other members of our laboratory for advice and support.

REFERENCES

1. Nicholson, A. W. (1999) *FEMS Microbiol. Rev. 23*, 371−390.
2. Grunberg-Manago, M. (1999) *Annu. Rev. Genet. 33*, 193−227.
3. Deutscher, M. P. (2000) *Prog. Nucleic Acid Res. Mol. Biol. 66*, 67−105.
4. Dunn, J. J. (1982) in *The Enzymes* (Boyer, P., Ed.) pp 485−499, Academic Press, New York.
5. Court, D. (1993) in *Control of Messenger RNA Stability* (Belasco, J. G., and Brawerman, G., Eds.) pp 71−116, Academic Press, New York.
6. Mian, I. S. (1997) *Nucleic Acids Res. 25*, 3187−3195.
7. Robertson, H. D., Webster, R. E., and Zinder, N. D. (1968) *J. Biol. Chem. 243*, 82−91.
8. Srivastava, A. K., and Schlessinger, D. (1990) *Annu. Rev. Microbiol. 44*, 105−129.
9. Robertson, H. D. (1982) *Cell 30*, 669−672.
10. Li, H., Chelladurai, B. S., Zhang, K., and Nicholson, A. W. (1993) *Nucleic Acids Res. 21*, 1919−1925.
11. Li, H., and Nicholson, A. W. (1996) *EMBO J. 15*, 101−113.
12. Zhang, K., and Nicholson, A. W. (1997) *Proc. Natl. Acad. Sci. U.S.A. 94*, 13437−13441.
13. Dunn, J. J. (1976) *J. Biol. Chem. 251*, 3807−3814.
14. Gross, G., and Dunn, J. J. (1987) *Nucleic Acids Res. 15*, 431−442.
15. Kharratt, A., Macia, M. J., Gibson, T. J., Nilges, M., and Pastore, A. (1995) *EMBO J. 14*, 3572−3584.
16. Fierro-Monti, I., and Mathews, M. B. (2000) *Trends Biochem. Sci. 25*, 241−246.
17. Rotondo, G., and Frendewey, D. (1996) *Nucleic Acids Res. 24*, 2377−2386.
18. Venclovas, C., and Siksnys, V. (1995) *Nat. Struct. Biol. 2*, 838−841.
19. Aravind, L., Makarova, K. S., and Koonin, E. V. (2000) *Nucleic Acids Res. 28*, 3417−3432.
20. Cowan, J. A. (1998) *Chem. Rev. 98*, 1067−1088.
21. Yang, D., Lu, H., and Erickson, J. W. (2000) *Curr. Biol. 10*, 1191−1200.
22. Bernstein, E., Caudy, A. A., Hammond, S. M., and Hannon, G. J. (2001) *Nature 409*, 363−366.
23. Dasgupta, S., Fernandez, L., Kameyama, L., Inada, T., Nakamura, Y., Pappas, A., and Court, D. L. (1998) *Mol. Microbiol. 28*, 629−640.
24. Grodberg, J., and Dunn, J. J. (1990) *J. Bacteriol. 170*, 1245−1253.
25. He, B., Rong, M., Lyakhov, D., Gartenstein, H., Diaz, G., Castagna, R., McAllister, W. T., and Durbin, R. K. (1997) *Protein Expression Purif. 9*, 142−151.
26. Perrin, S., and Gilliland, G. (1990) *Nucleic Acids Res. 18*, 7433−7438.
27. Amarasinghe, A. K., Calin-Jageman, I., Harmouch, A., Sun, W., and Nicholson, A. W. (2001) *Methods Enzymol*. (in press).
28. Kindler, P., Keil, T. U., and Hofschneider, P. H. (1973) *Mol. Gen. Genet. 126*, 53−69.
29. Nashimoto, H., and Uchida, H. (1985) *Mol. Gen. Genet. 201*, 25−29.
30. Milligan, J. F., Groebe, D. F., Witherell, G. W., and Uhlenbeck, O. C. (1987) *Nucleic Acids Res. 15*, 8783−8798.
31. Chakrabarti, P. (1990) *Protein Eng. 4*, 49−57.
32. Dunn, J. J., and Studier, F. W. (1983) *J. Mol. Biol. 166*, 477−535.
33. Chelladurai, B. S., Li, H., and Nicholson, A. W. (1991) *Nucleic Acids Res. 19*, 1759−1766.
34. Chelladurai, B. S., Li, H., Zhang, K. and Nicholson, A. W. (1993) *Biochemistry 32*, 7549−7558.
35. Reed, G. H., and Poyner, R. R. (2000) in *Metal Ions in Biological Systems* (Sigel, A., and Sigel, H., Eds.) Vol. 37, pp 183−207, Marcel Dekker, Inc., New York.
36. Keck, J. L., Goedken, E. R., and Marqusee, S. (1998) *J. Biol. Chem. 273*, 34182−34133.
37. Goedken, E. R., and Marqusee, S. (2001) *J. Biol. Chem.* (in press).
38. Lai, L., Yokota, H., Hung, L.-W., Kim, R., and Kim, S.-H. (2000) *Structure 8*, 897−904.
39. Dixon, M., and Webb, E. C., Eds. (1979) *Enzymes*, Academic Press, New York.
40. Fersht, A. (1985) *Enzyme Structure and Mechanism*, W. H. Freeman & Co., New York.

BI010022D